EUKARYOTIC CELL, May 2009, p. 703–712 Vol. 8, No. 5
1535-9778/09/$08.00+0 doi:10.1128/EC.00333-08

Live-Cell Imaging and Measurement of Intracellular pH in Filamentous Fungi Using a Genetically Encoded Ratiometric Probe▽†

Tanja Bagar,[1] Kirsten Altenbach,[2] Nick D. Read,[2] and Mojca Benčina[1]*

Department of Biotechnology, National Institute of Chemistry, Hajdrihova 19, SI-1000 Ljubljana, Slovenia,[1] and Fungal Cell Biology Group, Institute of Cell Biology, University of Edinburgh, Edinburgh EH9 3JH, United Kingdom[2]

Received 2 October 2008/Accepted 10 March 2009

A novel, genetically encoded, ratiometric pH probe (RaVC) was constructed to image and measure intracellular pH in living hyphae of *Aspergillus niger*. RaVC is a chimeric protein based on the pH-sensitive probe pHluorin, which was partially codon optimized for expression in *Aspergillus*. Intracellular pH imaging and measurement was performed by simultaneous, dual-excitation confocal ratio imaging. The mean cytoplasmic pH measured was 7.4 to 7.7 based on calibrating RaVC in situ within nigericin-treated hyphae. Pronounced, longitudinal cytoplasmic pH gradients were not observed in the apical 20 μm of actively growing hyphae at the periphery of 18-h-old colonies. The cytoplasmic pH remained unchanged after prolonged growth in buffered medium with pH values between 2.5 or 9.5. Sudden changes in external pH significantly changed cytoplasmic pH by <1.3 pH units, but it returned to its original value within 20 min following treatment. The weak acid and antifungal food preservative sorbic acid caused prolonged, concentration-dependent intracellular acidification. The inhibition of ATPases with *N*-ethylmaleimide, dicychlohexylcarbodimide, or sodium azide caused the cytoplasmic pH to decrease by <1 pH unit. Treatment with the protonophore carbonyl cyanide *m*-chlorophenylhydrazone or cyanide *p*-(trifluoromethoxy) phenylhydrazone reduced the cytoplasmic pH by <1 pH unit. In older hyphae from 32-h-old cultures, RaVC became sequestered within large vacuoles, which were shown to have pH values between 6.2 and 6.5. Overall, our study demonstrates that RaVC is an excellent probe for visualizing and quantifying intracellular pH in living fungal hyphae.

Cytoplasmic pH is a physiological parameter that is tightly regulated by a complex interaction of H^+ transport, H^+-consuming and -producing reactions, and H^+ buffering (10, 38). Maintaining pH within a physiological range is very important for protein stability, enzyme and ion channel activity, and many other processes that are required for cell growth, development, and survival (38). It has been proposed that intracellular pH serves as a mechanism by which cells coordinate the regulation of various processes that lack any other common regulating factors and may provide a link between the metabolic state and physiological responses (10).

The most reliable measurements of cytoplasmic pH in filamentous fungi in single living hyphae have indicated a pH of ~7.6. These measurements have been obtained using the ratiometric imaging of a dextran-conjugated, pH-sensitive dye injected into the cytoplasm to avoid sequestration into organelles (34). Changes in external pH were found to cause only small transient changes in the cytoplasmic pH, indicating that hyphae have a tightly regulated intracellular pH homeostatic mechanism. Rigorous quantitative analyses of cytoplasmic pH in growing hyphae and tip-growing plant cells have found no evidence for the existence of pronounced, tip-focused cytoplasmic pH gradients or for such gradients being required for the regulation of tip growth (4, 13, 34). These results contradicted previous reports of cytoplasmic pH gradients in hyphae (2, 25, 40, 41). Changes in cytoplasmic pH have been implicated in regulating protein synthesis, enzyme activities, and fermentation productivity in filamentous fungi (24) and cell cycle progression in fission yeast (26).

The recent sequencing and analysis of the genome of the filamentous fungus *Aspergillus niger* has revealed a complex machinery for H^+ transport that will play important roles in pH homeostasis and signaling (35). Key components of this machinery are five plasma membrane P-type H^+-ATPases; one vacuolar V-type H^+-ATPase; one mitochondrial membrane F_0F_1-ATP synthase; five K^+, Na^+/H^+ antiporters; and six Ca^+/H^+ antiporters (5).

Previous methods of measuring intracellular pH in filamentous fungi commonly have been fraught with problems. Loading hyphae with dextran-conjugated pH dyes or using pH-sensitive microelectrodes requires cells to be physically impaled with micropipettes or microelectrodes (42) and is technically demanding to perform without harming the cells under study (12, 33). Intracellular pH measurements with free pH-sensitive dyes often suffer from problems associated with dye loading and dye sequestration within organelles (21, 33). There are also reports on the use of radiolabeled membrane-permeable acids (3) and ^{31}P nuclear magnetic resonance (NMR) for intracellular pH measurement (18, 19, 20) in fungi. However, both of these methods require extensive sample manipulation and do not allow the imaging of intracellular pH in single living cells. Ideal probes for imaging and measuring intracellular pH in single living cells should possess several key

* Corresponding author. Mailing address: Department of Biotechnology, National Institute of Chemistry, Hajdrihova 19, SI-1000 Ljubljana, Slovenia. Phone: 38614760334. Fax: 38614760300. E-mail: mojca.bencina@ki.si.

† Supplemental material for this article may be found at http://ec.asm.org/.

▽ Published ahead of print on 13 March 2009.

properties. These include having a high selectivity for H^+ over other ions present; allowing the accurate quantification of intracellular pH; providing high temporal and spatial resolution; not interfering with normal physiological activities or cellular responses; exhibiting low cell toxicity; having a high signal-to-noise ratio; and having the possibility of being targeted to specific organelles.

A novel approach for noninvasive intracellular pH measurements has been the development of a recombinant pH-sensitive probe based on mutated green fluorescent protein (GFP) (6, 17, 29, 43). Miesenbock et al. (29) introduced a ratiometric pH probe of this type, which they named pHluorin. Problems normally encountered with single-wavelength dyes are reduced by using ratiometric probes. These problems include distinguishing between differences in intracellular pH and variations in dye brightness due to a variable intracellular dye concentration, dye photobleaching, or dye leakage from cells (33). Thus, pHluorin is very suitable as a noninvasive probe in living cells for imaging and measuring intracellular pH (26, 29, 43), but its use with filamentous fungi has not been reported previously.

The aims of this study were to (i) develop an improved version of the pHluorin probe (which we call RaVC) for intracellular pH imaging in filamentous fungi; (ii) obtain measurements of cytoplasmic pH in hyphae of *A. niger* expressing RaVC by using confocal ratio imaging; (iii) confirm or disprove that a pronounced, tip-focused, cytoplasmic pH gradient is absent in growing hyphae of *A. niger*; and (iv) assess the effects of changing the external pH, and of treating hyphae with known pH modulators, on intracellular pH homeostasis in *A. niger*.

MATERIALS AND METHODS

Strains, media, and growth conditions. *Aspergillus niger* A455 (*cspA1 pyrA6 leuA1 nicA1*) from the Microbial Culture Collection of the National Institute of Chemistry, Ljubljana, Slovenia, was used for transformation. Conidia were harvested from 4-day-old agar slants and suspended in sterile 0.1% Tween-80 solution. A conidial suspension (approximately 5×10^7 ml^{-1}) was used for inoculating 100 ml of complete medium with the following composition: minimal medium, 0.1% (wt/vol) yeast extract, 0.1% (wt/vol) Casamino Acids, and 2% (wt/vol) glucose. The composition of the minimal medium was 71 mM $NaNO_3$, 11 mM KH_2PO_4, 6.7 mM KCl, 2 mM $MgSO_4 \cdot 7H_2O$, pH 6.0, 0.2 ml trace metal solution [34.3 mM EDTA, 15.3 mM $ZnSO_4 \cdot 7H_2O$, 8 mM $MnCl_2 \cdot 4H_20$, 1.6 mM $CoCl_2 \cdot 6H_2O$, 1.3 mM $CuSO_4 \cdot 5H_2O$, 0.2 mM $(NH_4)_6Mo_7O_{24} \cdot 4H_20$, 10 mM $CaCl_2 \cdot 2H_2O$, 3.6 mM $FeSO_4 \cdot 7H_2O$; pH 6.5]. The fungus was incubated in 500-ml baffled Erlenmeyer flasks on a rotary shaker at 100 rpm and 30°C. For imaging, fungi were grown in liquid Vogel's medium with the following composition: 8.5 mM sodium citrate dihydrate [$Na_3(C_6H_5O_7)$], 36.8 mM KH_2PO_4, 25.0 mM NH_4NO_3, 0.7 mM $CaCl_2 \cdot 2H_2O$, 0.8 mM $MgSO_4 \cdot 7H_2O$, pH 6.0, 0.2 ml trace metal solution, 20 μM D-biotin, and 2% (wt/vol) glucose. All mutant strains were grown on medium with 0.08 mM nicotinamide, 1.5 mM leucine, and 5 mM uridine if required for auxotrophic growth. *Escherichia coli* DH5α (New England Biolabs) was used for plasmid DNA propagation, and *E. coli* BL21(DE3) (Novagen) was used for protein expression. *E. coli* cells were grown using standard Luria-Bertani broth in a shaker incubator at 37°C overnight. The induction of protein was initiated with the addition of 0.4 mM isopropyl-β-D-thiogalactopyranoside. pGW635 containing the *A. niger* orotidine-5-phosphate decarboxylase (*pyrA*) gene was used as a selection marker for the fungal transformation.

RaVC gene construction. A pH-sensitive GFP named RaVC was constructed based on the template of ratiometric pHluorin (29). Substantial codon optimization for *Aspergillus* was achieved by using fragments of Citrine (15) and Venus (39) to replace segments of pHluorin that did not encode amino acid residues conferring pH sensitivity to the probe (see the supplemental material for further details). For expression in *A. niger*, the RaVC gene was subcloned into the pMOJ009 vector, using restriction sites NdeI and EcoRI, where it was expressed under the control of the strong constitutive glyceraldehyde phosphate dehydrogenase (*gpdA*) promoter of *Aspergillus nidulans* and the anthranilate synthase (*trpC*) terminator of *A. nidulans*.

Fungal transformation. For the transformation of *A. niger*, mycelium was prepared by incubating conidia for 16 to 18 h in liquid culture in complete medium with appropriate supplements. The protoplasts were prepared by treating mycelia (1 g) with 10 μg/ml caylase C4 dissolved in 20 ml KMC buffer (1 M KCl, 25 mM $CaCl_2$, 10 mM Tris, pH 5.8) for 1 to 3 h. Protoplasts were collected by centrifugation for 10 min at 4,000 × *g* at 4°C and washed twice with 5 ml cooled STC (1.33 M sorbitol, 50 mM $CaCl_2$, 10 mM Tris, pH 7.5). For the cotransformation of *A. niger* A455, 1 μg pGW635 DNA and 5 μg of the cotransforming plasmid RaVC were added to 2×10^7 protoplasts in 0.2 ml STC buffer. A mixture of protoplasts and DNA was treated with 50 μl of polyethylene glycol [PEG] buffer (25% PEG 600, 50 mM $CaCl_2$, 10 mM Tris, pH 7.5) for 20 min at room temperature. Two milliliters of PEG buffer was added to the mixture, and the mixture was incubated at room temperature for 5 min. Finally, the transformation procedure was stopped with the addition of 5 ml STC buffer. This mixture was added to 30 ml MMS agar (0.7% [wt/vol] 71 mM $NaNO_3$, 11 mM KH_2PO_4, 6.7 mM KCl, 2 mM $MgSO_4 \cdot 7H_2O$, pH 6.0, 0.2 ml trace metal solution, 2% [wt/vol] glucose, 0.95 M sucrose) and poured on MMS plates (1.5% [wt/vol] agar). The transformants were selected and purified by replating at low conidial densities on selective medium.

In vitro characterization of RaVC. For in vitro characterization, the protein was expressed in *E. coli* BL21(DE3) cells. Cells were resuspended in 10 mM Tris, 1 mM EDTA, 0.7 to 1.4 mM lysozyme and sonicated for 9 min on ice, with a repeated 1-s ultrasound pulse followed by a 2-s pause (Tekmar sonic disruptor). The cell lysate was centrifuged, and the supernatant was used for in vitro analysis. The partially purified RaVC probe was resuspended in buffers with different defined pH values. Spectral characteristics of the RaVC protein were determined using a spectrophotometer (Perkin Elmer LS 55) with excitation in the range of 350 to 500 nm (with a 5-nm bandwidth) and emission detected at 508 nm (with a 5-nm bandwidth). The emission intensities of the two major emission peaks, 395 and 475 nm, were determined. The ratios calculated from the intensities of the two emission peaks (see equations 1 and 2) were plotted as a function of pH.

In situ calibration of RaVC. For the in situ recording of fluorescence ratios within hyphae, 100-μl drops of Vogel's medium containing *A. niger* conidia (10^5 ml^{-1}) were incubated on a coverslip in a humid chamber for ~18 h prior to imaging. During this period, the conidia germinated and a mycelium was formed. A calibration curve was obtained by incubating mycelia in buffer solutions with different pH values, ranging from 5.0 to 9.0, with freshly prepared 5 μM nigericin. The ionophore nigericin was used to equilibrate the intracellular pH with the extracellular pH, and the treated mycelia were given at least 30 min to reach this state (23, 24). The following buffers were used at a concentration of 50 mM, with 150 mM KCl added: acetate (pH 5.0 to 5.5), morpholineethanesulfonic acid (pH 6.0 to 6.75), morpholinepropanesulfonic acid (pH 7.0 to 7.8), and Tris (pH 8.0 to 9.0). After mycelia had been treated for 30 min with nigericin, fluorescence intensities after excitation at 405 and 476 nm on the confocal microscope were recorded at 5-min intervals, and ratios were calculated. Ten minutes after the mean ratio reached a steady state, it was converted to a pH value using equation 1.

Confocal laser-scanning microscopy. A Leica TCS SP5 laser-scanning microscope mounted on a Leica DMI 6000 CS inverted microscope (Leica Microsystems, Germany) with an HCX plan apo ×63 (numerical aperture, 1.4) oil immersion objective was used. For sequential excitation, a 50-mW, 405-nm diode laser and the 476-nm line of a 25-mW argon laser were used. Laser powers of 6% for the diode laser and 12% for the argon laser were employed. Successive images excited at 405 and 476 nm were captured within 1.2 s of each other. Fluorescence emission was detected at 500 to 530 nm. SynaptoRed 2 (Biotium) was excited with the 514-nm line of the argon laser, and its fluorescence was detected at 650 to 700 nm.

Calibration of intracellular pH. Images were analyzed using either the ImageJ plugin PixFret (9) or a software program custom written for this application and incorporating equations 1 and 2, which are described below. Ratio images were obtained by first subtracting the background from each fluorescence image pair followed by the division of corresponding pixels in the image pair:

$$R_i = (F_{405\text{ nm i}} - F_{405\text{ nm background}})/(F_{475\text{ nm i}} - F_{475\text{ nm background}}) \quad (1)$$

where R_i is the emission ratio at a given pH, $F_{405\text{ nm i}}$ and $F_{475\text{ nm i}}$ are the fluorescence intensities of a given image pixel or region of interest, and $F_{405\text{ nm background}}$ and $F_{475\text{ nm background}}$ are average background fluorescence intensities of a given pixel or region of interest. The ratio of fluorescence signals emitted at each excitation wavelength was converted to pH values (see equation

2) (7, 16). The experimental data were analyzed by fitting the following equation to the calibration curve:

$$pH = pK_a - \log_{10}[(R_i - R_{min})/(R_{max} - R_i)] \quad (2)$$

where R_{max} and R_{min} are the limiting values for the ratio at the extreme acid (pH 5.0) and alkaline (pH 9.0) pH values, respectively; they were determined individually for each set of experiments. The constant pK_a was determined from the in situ calibration curve. Visually, the pH profile along the hyphae was expressed by converting the gray scale of the ratio image into pseudocolors. All data are shown as the means with standard deviations from at least three independent experiments, and a minimum of three images were taken for each experiment. To reduce noise in the ratio images resulting from noise in the original two images used to create the ratio images, the cytoplasm was divided into 0.2- by 0.2-μm-sized sectors and the average ratio was calculated in each sector. Although this reduced the noise, it resulted in some artifactual inhomogeneity in the appearance of the cytoplasm in the ratio images (see Fig. 4C). Mean pH values were calculated from cytoplasmic areas that excluded detectable organelles or cytoplasmic regions in which the RaVC reporter was concentrated.

Chemical treatments applied to living hyphae. Fungi were mostly grown in Vogel's medium with appropriate supplements. The only exception was the experiment in which the effect of the external pH on the intracellular pH was assessed. Here, pH-adjusted minimal medium was used, because salts in Vogel's medium were precipitated at low pH. All chemicals were prepared as 10× stock solutions in appropriate solvents. The solvents were found not to have an effect on intracellular pH (data not shown). The extracellular pH was changed by the addition of 5 mM KOH or 50 mM HCl to Vogel's medium, and the responses of intracellular pHs were monitored for 20 min. The inhibition of ATPases was achieved with 100 μM dicychlohexylcarbodimide (DCCD; Sigma), 100 μM *N*-ethylmaleimide (NEM; Sigma), 1 mM sodium vanadate (Na_2VO_4), or 1 mM sodium azide (NaN_3). Oxidative phosphorylation was inhibited using 10 μM carbonyl cyanide *m*-chlorophenylhydrazone (CCCP; Fluka) or 40 μM cyanide *p*-(trifluoromethoxy) phenylhydrazone (FCCP; Sigma). The effect of sorbic acid on the intracellular pH was monitored using 5 or 10 mM sorbic acid. For each chemical treatment, images were captured before treatment and for 10 min following chemical addition.

Availability of materials. The *A. niger* RaVC transformants are freely available from the Microbial Culture Collection of the National Institute of Chemistry. All other novel material described in this paper can be obtained for noncommercial purposes on request from the corresponding author.

RESULTS

Codon optimization was used to improve RaVC expression. There have been reports of reduced GFP expression in *Aspergillus* due to nonoptimal codon usage (11). Using codon usage data (31 and CUTG Codon usage tabulated from the NCBI-GenBank Flat File, release 156.0 [15 October 2006; http://www.kazusa.or.jp/codon/]), codon usage in native pHluorin and *A. niger* was compared by calculating the percentage that codons were used for each amino acid (see Table S2 in the supplemental material). This analysis showed that pHluorin contains 46 codons that are rare in *A. niger* (used 15% or less) and strongly suggested the need for codon optimization to achieve a good expression of the heterologous gene in *A. niger*.

A synthetic, codon-optimized ratiometric pH-sensitive GFP was constructed as described in the supplemental material. Amino acids 132, 147, 149, 164, 166, 167, 168, 202, and 220 are responsible for the ratiometric nature and spectral characteristics of pHluorin (29) and thus were preserved (see Fig. S1 in the supplemental material). Substantial codon optimization was achieved by replacing some fragments of the pHluorin gene with complementary fragments from Citrine or Venus genes; Venus (39) and Citrine (15) are improved yellow fluorescent proteins that have been shown to be expressed well in *A. niger* (30). We also introduced a point mutation at amino acid site 206, replacing alanine with lysine (47), to create a monomeric RaVC variant. Codon optimization reduced the number of rare codons in RaVC from 46 to 19.

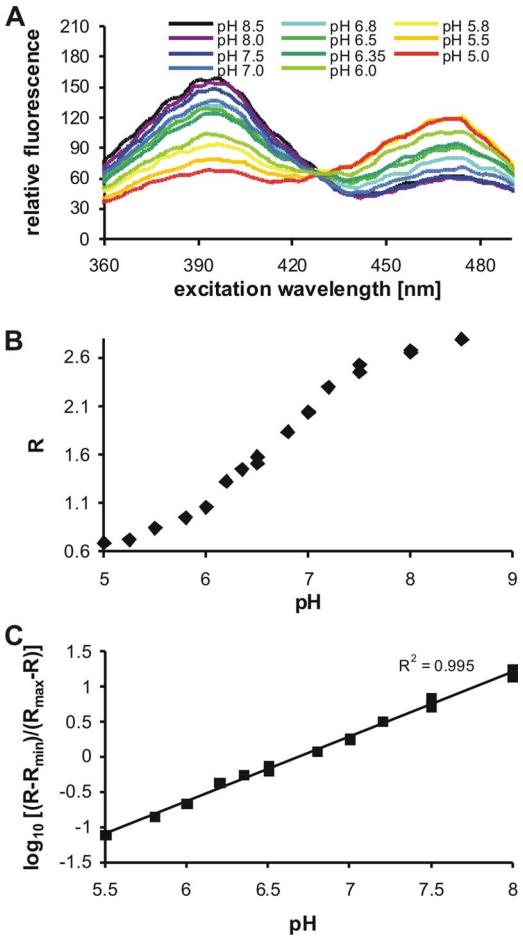

FIG. 1. Fluorescent properties of the genetically encoded ratiometric probe RaVC. (A) Fluorescence excitation spectra of RaVC in various pH-adjusted buffers were determined with a spectrofluorimeter. Samples containing partially purified RaVC in a solution were excited at between 350 ± 2.5 and 500 ± 2.5 nm, and the fluorescence emission was collected at 508 ± 2.5. (B) In vitro calibration curve of RaVC presented as a plot of the fluorescence excitation ratio versus pH. The ratio (R) between the emission intensities after excitation at excitation maxima of 395 and 475 nm were calculated using equation 1. The emission intensities were obtained from fluorescence spectra presented in panel A. (C) In vitro calibration curve of RaVC presented as a logarithmic plot of the fluorescence excitation ratio (B) versus pH.

In vitro calibration demonstrates pH sensitivity and spectral characteristics of RaVC. The recombinant pH probe RaVC was expressed in both *E. coli* and *A. niger*. The protein was partially purified and its spectral sensitivity to pH was assessed, first in vitro in solution and then in situ within fungal hyphae. Excitation spectra of partially purified RaVC in buffers of defined pH are shown in Fig. 1A. RaVC has pH-dependent spectra with an isosbestic point at 42 ± 3 nm, excitation maxima at 395 ± 4 and 475 ± 2 nm, and an emission maximum at 508 ± 2 nm. The linear response of RaVC to pH is between pH 5.5 and 8.0 (Fig. 1B). Emission intensities detected after 395- and 475-nm excitation, at pH 5.0 and 8.5, were used to calculate the minimum and maximum ratios. These data are included in equations 1 and 2 for pH determination (see Ma-

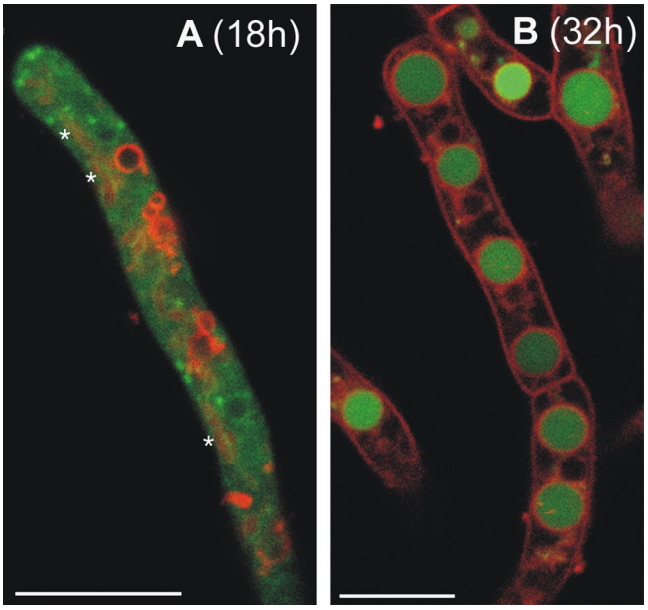

FIG. 2. Age-dependent distribution of RaVC in living hyphae. The hyphae grown in liquid culture were imaged by confocal microscopy either 18 (A) or 32 h (B) after inoculation. The two figures are of merged images showing pH-dependent RaVC fluorescence (green) and the localization of membrane-selective probe SynaptoRed 2 fluorescence (red). Note that RaVC is localized in the cytoplasm in 18-h-old hyphae (A) and is mostly localized in large putative vacuoles in 32-h-old hyphae (B). Tubular vacuoles in panel A are indicated by asterisks; they are not as clear as the labeled membranes of the spherical vacuoles. Bars = 7.5 (A) and 10 μm (B).

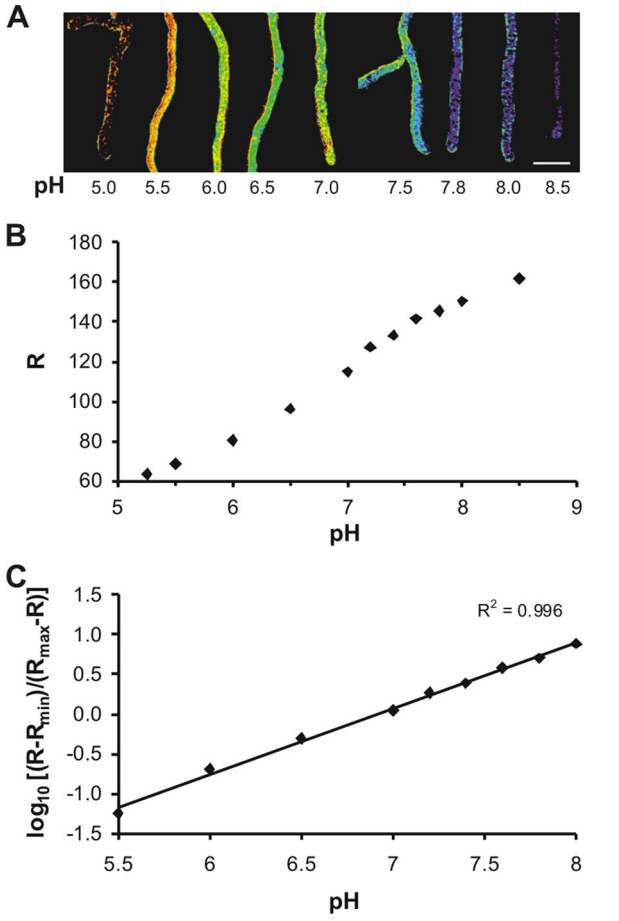

FIG. 3. In situ calibration of RaVC. (A) Pseudocolored images of *A. niger* expressing RaVC. Different colors have been assigned to defined pH values according to the in situ calibration curve calculated with equation 2 and shown in panel B. Scale bar = 10 μm. (B) A plot of the fluorescence excitation ratio versus intracellular pH. Eighteen-hour-old *A. niger* cells expressing RaVC were washed with pH-adjusted buffers and treated with freshly prepared nigericin to equalize the extracellular pH with the intracellular pH. The ratio (R) between the emission intensities (collected between 500 and 530 nm) after excitation at 405 and 476 nm for each image pixel in hyphae was calculated using equation 1. Measurements were performed by sequential dual-excitation confocal imaging. (C) A logarithmic plot of the fluorescence excitation ratio (B) versus intracellular pH.

terials and Methods). The pK_a determined in vitro for RaVC was 6.7 (Fig. 1B).

In situ calibration allows determination of intracellular pH. After the visualization by confocal microscopy of hyphae grown in liquid medium, RaVC probe was expressed in *A. niger* and found to be localized mainly in the cytoplasm of growing hyphae in 18-h-old colonies (Fig. 2A). These young hyphae possessed spherical and tubular organelles that had morphologies characteristic of vacuoles when labeled with the membrane-selective dye SynaptoRed 2 (also called FM4-64), which stained the vacuolar membranes (21, 22). These putative vacuoles did not take up RaVC in 18-h-old colonies (Fig. 2A). However, RaVC did become concentrated in small spherical organelles/cytoplasmic domains that did not clearly label with SynaptoRed 2 (Fig. 2A). In nongrowing hyphae of 32-h-old cultures, much of the RaVC became sequestered in larger spherical organelles, which were presumed to be vacuoles (Fig. 2B).

The presence of RaVC, and the laser irradiation required to generate up to 10 ratio images per min, had no discernible influence on fungal physiology. The growth and branching patterns of hyphae appeared normal, and the extension rates of RaVC-expressing strains were similar to those of untransformed strains (unpublished results).

An in situ calibration was performed to accurately determine the cytoplasmic pH in living hyphae. Fungal hyphae were permeabilized with nigericin in the presence of buffers with different pH values. Images were collected (Fig. 3A), and ratios of emission intensities detected after excitation at 405 and 476 nm were calculated based on equation 1 (R_{min} and R_{max} were calculated from the emission intensities at pH 5.0 and 8.5). The in situ calibration clearly shows that RaVC displays pH sensitivity in the normal physiological range within living hyphae. A logarithmic plot of the standard curve is presented in Fig. 3B. The pK_a determined in situ for RaVC is 6.9 ± 0.1, and its optimal linear response to pH is between pH 5.5 and 8.0 (Fig. 3B). The pK_a as well as R_{min} and R_{max}, which were determined for each set of experiments separately, were used to calculate the intracellular pH within hyphae pixel by pixel using equation 2.

The mean value for cytoplasmic pH in growing hyphae from 18-h-old colonies was 7.6 ± 0.1 and varied between pH 7.4 and 7.7. Mean pH values were calculated from cytoplasmic areas

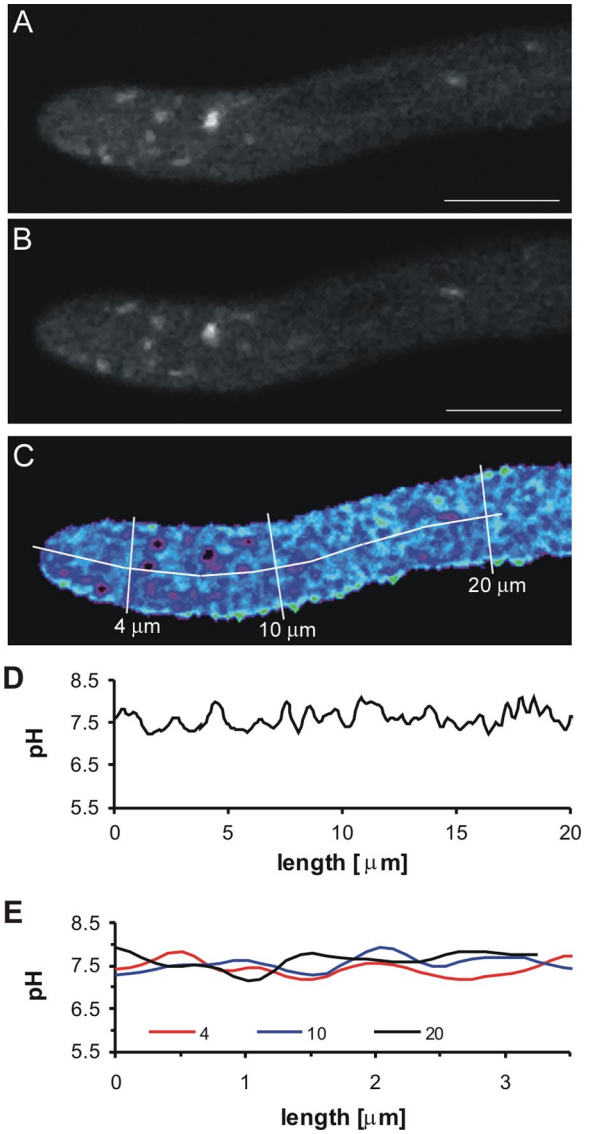

FIG. 4. Intracellular pH analysis of a growing hyphal tip expressing RaVC from the margin of an 18-h-old colony. The images are median optical sections through the hyphal tip and were captured sequentially. (A) Image of RaVC fluorescence (500 to 530 nm) after excitation at 405 nm. (B) Image of RaVC fluorescence (500 to 530 nm) after excitation at 476 nm. (C) Pseudocoloured ratio image of the fluorescence intensities of RaVC after a pixel-by-pixel calculation using equations 1 and 2 (see Materials and Methods). Black intracellular regions represented regions in which the fluorescent signal was saturated, preventing the accurate determination of intracellular pH. (D) Intracellular pH along the longitudinal transect shown in panel C. (E) Intracellular pH along the transverse transects shown in panel C. Bar = 5 μm.

that excluded detectable organelles or cytoplasmic regions in which the RaVC reporter was concentrated. The pH of the putative vacuoles in the older nongrowing hyphae of 32-h-old colonies varied between 6.2 and 6.5. The average pH of the small spherical organelles/cytoplasmic domains that did not appear to be membrane bound but within which the probe was concentrated (Fig. 2A and 4A and B) was also determined and found to be above 8 in most cases. However, the fluorescent signal in these bright regions was frequently saturated, preventing accurate pH measurement. Intracellular regions in which the fluorescent signal was saturated appeared black in the ratio images (Fig. 4A to C).

Pronounced tip-focused, cytoplasmic pH gradient cannot be detected in growing hyphal tips. The association of a pronounced tip-focused, cytoplasmic pH gradient in the apices of tip-growing cells has been controversial (13, 25, 34). To determine whether pH gradients of this type can be visualized in unperturbed, growing hyphal tips of *A. niger*, we analyzed the cytoplasmic pH along and across growing hyphae expressing RaVC.

Ratio images of growing hyphae expressing RaVC from 18-h-old cultures were captured, and their cytoplasmic pH values were determined (Fig. 4A to C). The extension rates of these hyphae were between 0.5 and 0.8 μm min^{-1}. The plasma membrane was stained with the dye SynaptoRed 2 to visualize the cytoplasmic boundary (not shown). Although minor fluctuations in the cytoplasmic pH were observed, no obvious cytoplasmic pH gradient could be detected along the lengths of growing hyphae (Fig. 4D) or in cross-sections at different distances from their tips (Fig. 4E).

Cytoplasmic pH remains unperturbed after prolonged exposure to extreme external pH. *Aspergillus niger* is able to grow at extreme external pH values (20, 24, 27). Our results show that conidia of *A. niger* expressing RaVC were able to germinate, and hyphae grew in media with pH values between 2.5 and 9.5 (Fig. 5A). The greatest mycelial growth after 18 h at 30°C was observed at pH 5.5. At pH 9.5, the mycelial dry weight was reduced by 50%, and at pH 2.5 it was reduced by 70% (Fig. 5A). Fluorescence ratio imaging showed that hyphae grown at pH 2.5 to 9.5 were able to maintain their cytoplasmic pH at 7.6 (Fig. 5B). Cytoplasmic pH gradients were not detected under any of these conditions.

Cytoplasmic pH recovers in response to sudden changes in external pH. The results described above show that *A. niger* possesses a robust machinery for intracellular pH homeostasis, allowing the fungus to germinate and grow in the presence of low or high external pH. We next addressed the question of what effects sudden changes of extracellular pH would have on cytoplasmic pH. The addition of the strong acid HCl (50 mM) or the strong base NaOH (5 mM) to growing hyphae resulted in a transient acidification or alkalinization of the cytoplasm, respectively (Fig. 6A and B). Thirty seconds after the addition of HCl, the cytoplasmic pH transiently dropped from 7.6 ± 0.1 to 6.3 ± 0.2 uniformly along hyphae. Similarly, the addition of NaOH transiently increased the cytoplasmic pH from 7.6 ± 0.1 to 8.3 ± 0.1. The cytoplasmic pH returned to its homeostatic pH value (7.4 to 7.7) within 20 min. The addition of 50 mM HCl or 5 mM NaOH resulted in the pH of the extracellular medium changing by 3.5 or 0.5 pH units, respectively.

Sorbic acid causes prolonged intracellular acidification. It has been proposed that the preservative sorbic acid inhibits conidial germination and mycelial growth through intracellular acidification, because it is a weak cell-permeant acid (36). Growing hyphae were treated with 5 or 10 mM sorbic acid (Fig. 6C and D). The cytoplasmic pH was measured prior to the addition of sorbic acid and then monitored for 30 min. The sorbic acid treatments resulted in a concentration-dependent cytoplasmic acidification. Sorbic acid (10 mM) caused an acid-

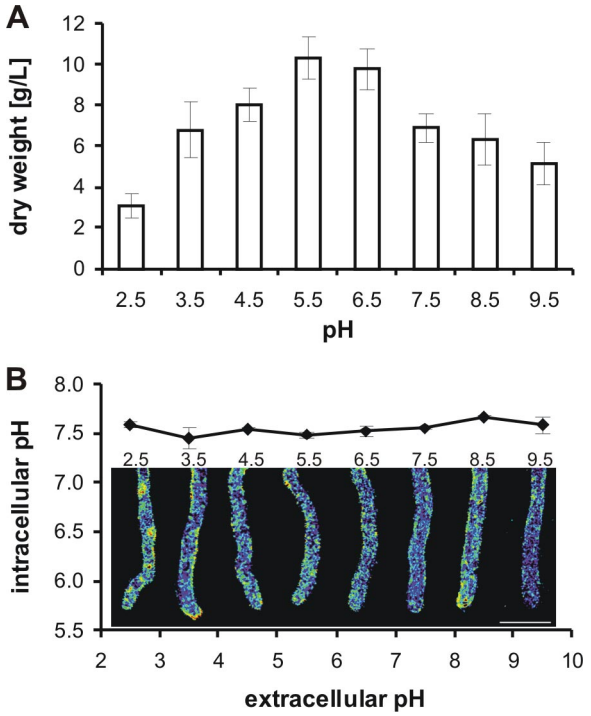

FIG. 5. Influence of external pH on cytoplasmic pH. (A) Growth of mycelium at 30°C in liquid minimal media with defined pH values. Eighteen hours after spore inoculation (10^6 spores ml^{-1}), mycelia were collected and their biomass was determined gravimetrically after the washed mycelia were dried at 105°C to a constant weight. (B) The average cytoplasmic pH values with representative ratio images from growing hyphae expressing RaVC from the periphery of 18-h-old cultures grown in minimal media with pH values between 2.5 and 9.5. Cytoplasmic pH values were calculated from the fluorescence ratios using the in situ calibration, and the pseudocolors selected represent cytoplasmic pH values between 7.5 and 7.7. Mean cytoplasmic pH values (± standard deviations) for each ratio image also are shown. Bar = 10 μm.

ification from pH 7.5 ± 0.1 to 5.9 ± 0.3 within 1 min of addition, and the cytoplasmic pH did not recover even after 30 min. The addition of 5 mM sorbic acid resulted in a slower and less significant decrease in cytoplasmic pH, from 7.5 ± 0.1 to 6.6 ± 0.1, and again this change in intracellular pH was for longer than 30 min.

Agonists of pH homeostasis decrease cytoplasmic pH. Various known H^+-ATPase inhibitors and inhibitors of oxidative phosphorylation were tested to determine their effects on intracellular pH homeostasis. We tested the effects of the H^+-ATPase inhibitors DCCD (100 μM), NEM (100 μM), sodium vanadate (1 mM), and sodium azide (1 mM), and two protonophores, CCCP (10 μM) and FCCP (40 μM), also known as uncouplers of oxidative phosphorylation (14). The pharmacological agents were added to 18-h-old growing hyphae, and the dynamic changes in the cytoplasmic pH were measured before and after the addition of the chemicals by the fluorescence ratio imaging of RaVC.

We observed different effects of the pH agonists on the cytoplasmic pH (Fig. 7). The strongest effect was observed using 100 μM DCCD and 1 mM sodium azide, where the cytoplasmic pH dropped from 7.6 to 5.6 in 1 min and did not recover to its original value within 10 min (Fig. 7A and C). The addition of 1 mM sodium vanadate had no effect on the cytoplasmic pH (Fig. 7A and C). We also tested if 1 mM sodium vanadate would influence the cytoplasmic pH if it was present in the medium at the time of inoculation and found that the cytoplasmic pH in growing hyphae from 18-h-old treated cultures was 0.2 pH units lower than normal (data not shown).

Both of the protonophores FCCP and CCCP caused the acidification of the cytoplasmic pH, which did not recover within 10 min of agonist addition. After 5 min, 10 μM CCCP reduced the cytoplasmic pH from 7.6 to 6.0, and 40 μM FCCP reduced the cytoplasmic pH more rapidly, from 7.6 to 5.6 (Fig. 7B and C).

DISCUSSION

GFP-based pH sensors have proven immensely valuable for studies of intracellular pH in higher eukaryotes (46). Because of difficulties in using fluorescent dyes to image and measure intracellular pH in filamentous fungi (33), we developed and successfully used a novel genetically encoded pH sensor, which we have called RaVC. The codon-optimized, ratiometric RaVC probe was found to possess excellent properties for

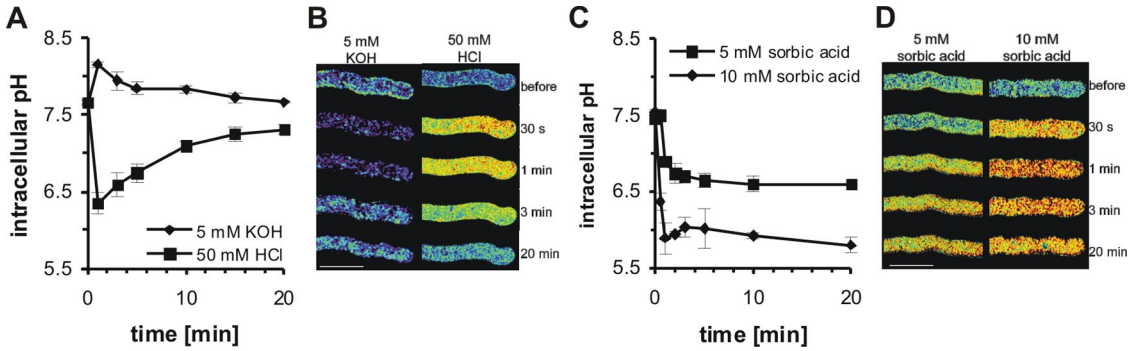

FIG. 6. Response of cytoplasmic pH to a sudden extracellular pH change. Cytoplasmic pH measurement and fluorescence ratio imaging of cytoplasmic pH in growing hyphae expressing RaVC from 18-h-old cultures. (A) Effects of a strong acid (50 mM HCl) or base (5 mM KOH) on cytoplasmic pH. (C) Effects of sorbic acid (5 or 10 mM) on cytoplasmic pH. (B and D) Pseudocolored fluorescence ratio images of hyphae. The pseudocolors correspond to defined pH values calculated from the fluorescence ratios using the in situ calibration (blue, alkaline; red, acidic). Bars = 10 μm.

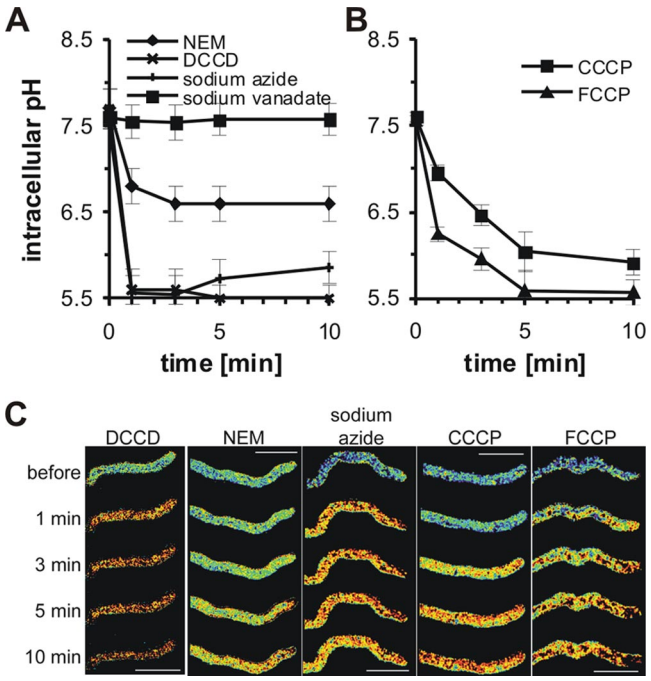

FIG. 7. pH agonists decrease cytoplasmic pH. Shown are the cytoplasmic pH measurements and fluorescence ratio images of cytoplasmic pH in growing hyphae expressing RaVC from 18-h-old cultures. (A) Acidification by ATPase inhibitors DCCD (0.1 mM), NEM (0.1 mM), sodium azide (1 mM), and sodium vanadate (1 mM). (B) Acidification by the oxidative protonophores/phosphorylation inhibitors CCCP (10 μM) and FCCP (40 μM). (C) Pseudocolored fluorescence ratio images of hyphae treated with the pH agonists. The pseudocolors correspond to defined pH values calculated from the fluorescence ratios using the in situ calibration (blue, alkaline; red, acidic). Bars = 10 μm.

visualizing and quantifying intracellular pH in growing hyphae of *A. niger*. Hyphae of *A. niger* were shown to have a tightly regulated pH homeostatic mechanism, and H^+-ATPases were demonstrated to play an important role in maintaining the cytoplasmic pH between 7.4 and 7.7, with a mean pH of 7.6 ± 0.1. Pronounced, tip-focused cytoplasmic pH gradient could not be detected in growing hyphae. Vacuoles in older hyphae expressing RaVC were found to have pH values between 6.2 and 6.5.

Why RaVC is an excellent pH sensor for filamentous fungi. RaVC has a number of properties that make it an excellent pH sensor for filamentous fungi. These properties include (i) it is genetically encoded; (ii) it allows the accurate quantification of intracellular pH with high spatial and temporal resolution; and (iii) it has low toxicity and does not interfere with normal physiological processes.

RaVC is genetically encoded, which avoids the necessity for physical perturbation or manipulation to introduce the pH sensor into a cell. The gene encoding pHluorin (29) was partially codon optimized to improve its level of expression, with the result that RaVC produced a strong fluorescent signal within the fungal cells. The codon optimization involved reducing the number of rare codons from 46 to 19 but preserved all of the amino acids that conferred the ratiometric characteristics and defined the spectral properties of the original pHluorin (29). We additionally replaced alanine 206 with lysine to reduce the tendency of GFP to dimerize (47). Codon optimization has been used previously in filamentous fungi to improve the level of expression of GFP (11) and the bioluminescent calcium sensor aequorin (32). Although RaVC was constitutively expressed in the cytoplasm of *A. niger* in this study, because it is genetically encoded it can be easily targeted to different organelles to measure organellar pH in future studies.

RaVC has excellent spectral characteristics in vitro and in situ within the fungal cell that allow for the accurate quantification of intracellular pH with high spatial and temporal resolution. Important spectral characteristics of RaVC measured in vitro are as follows. (i) Its excitation peaks (395 and 475 nm) are pH dependent, allowing it to be used as a dual-excitation, ratiometric dye. These two excitation wavelengths relate to the protonated and deprotonated states, respectively, of tyrosine 67, which forms a part of the chromophore (29). (ii) Its isosbestic point (i.e., the excitation wavelength that is pH independent) is 428 nm. Excitation at this wavelength can be useful to determine the concentration of RaVC in different regions of a cell (8). (iii) Its maximum fluorescence is at 508 nm (i.e., in the visible, blue-green part of the light spectrum). (iv) The linear range of the fluorescence ratios of the probe is between pH 5.5 and 8.0. This pH range, over which the sensor is most pH sensitive, is also the range within which most intracellular pH values of physiological significance reside. (v) The dynamic range of pH-dependent fluorescence ratios of RaVC is large, allowing the precise quantitation of pH with a high signal-to-noise ratio. The in vitro spectral characteristics of RaVC were very similar to the original pHluorin (29) from which it was derived, indicating that the modifications we had made did not alter its spectral properties or pH sensitivity.

The spectral properties of RaVC determined in vitro showed only small differences with those measured in situ. For the in situ calibration curve, young *A. niger* hyphae expressing RaVC were permeabilized with the K^+/H^+ ionophore nigericin (23, 24) in the presence of buffers with different pH values. Nigericin was used to equalize the cytoplasmic pH with the external pH. The in situ calibration showed that the RaVC expressed inside fungal cells could be used to measure intracellular pH across the physiological range of pH 5.5 and 8.0. The pK_a of RaVC inside fungal cells was shown to be 6.9; in vitro it was 6.7. This slight shift in pK_a probably is due to differences between the intracellular environment and the in vitro calibration solutions. The ionic strength, viscosity, and hydrophobicity of the medium and the dyes all have been identified as potential factors that influence the response of ion-sensitive dyes (12). A similar shift of pK_a also was reported for pH-sensitive GFP expressed in plants (43). To visualize the spatial distribution of pH within hyphae, fluorescence ratio images and, consequently, pH values were calculated pixel by pixel using equations 1 and 2 (see Materials and Methods) (7, 16).

RaVC was localized in the cytoplasm in young hyphae from 18-h-old colonies and became sequestered within putative vacuoles in older hyphae from 32-h-old colonies. However, its cytoplasmic distribution was nonuniform and concentrated in certain regions (organelles or cytoplasmic domains), which could not be identified. These regions were not surrounded by

the membrane-selective dye SynaptoRed 2 (also known as FM4-64). Whether these regions were membrane bound or not is unclear, because not all membranes are labeled with SynaptoRed 2 (21). However, it was evident that these intracellular regions possessed a more alkaline pH than the surrounding cytoplasm, although their precise pH could not be determined.

No toxic side effects or physiological perturbation of hyphae expressing RaVC was observed. In particular, the growth and branching patterns of hyphae appeared normal, and the extension rates of RaVC-expressing strains were similar to those of untransformed strains.

Cytoplasmic pH is tightly regulated by a robust pH homeostat. Our study revealed that the cytoplasmic pH in young hyphae of *A. niger* is tightly regulated at pH ~7.6. This estimate is in agreement with intracellular pH measurements obtained with ^{31}P-NMR (19, 36), but it was 0.2 pH units higher when measurements were made with the ratiometric fluorescent dye SNARF (24). However, in the latter study an esterified version of the SNARF dye was used that tends to sequester within intracellular organelles (34). When Parton et al. (34) compared measurements of cytoplasmic pH in hyphae of *Neurospora crassa* obtained with esterified SNARF and a dextran-conjugated SNARF, which exhibits superior localization and retention within the cytoplasm, they found that the former provided cytoplasmic pH values of 7.2 and the latter provided cytoplasmic pH values of 7.6 (which is consistent with our results). It thus appears likely that RaVC provides accurate measurements of cytoplasmic pH in young hyphae of *A. niger*. However, it is also clear that the high-resolution, ratiometric imaging of hyphae expressing RaVC needs to be performed to discriminate between fluorescence from the cytoplasm and that from the unidentified cytoplasmic domains/non-membrane-bound organelles within which RaVC became sequestered, because the latter will bias the average intracellular pH to more alkaline values.

The existence of a robust pH homeostat in hyphae of *A. niger* has been reported previously (20). Our results show that the cytoplasmic pH is maintained at ~7.6 even when the external pH ranges from 2.5 to 9.5. *Aspergillus niger* is used for citric acid production (20, 24, 27), and excreted citric acid can acidify its growth environment down to pH 1.5. This organism therefore needs a robust homeostatic mechanism to maintain the cytoplasmic pH at a constant value in order for its cells to survive and function in extreme pH environments. Plasma membrane H^+-ATPases play a major role in intracellular pH homeostasis (20) and will be most active in extreme pH environments. Perhaps the increased activity of H^+-ATPases reduces the intracellular ATP pool in hyphae growing under these conditions and contributes to a reduced growth rate because of the limited amount of ATP available for other cellular activities (e.g., metabolism and nutrient uptake).

Intracellular pH was found to recover within 20 min following the addition of a strong acid or base. This demonstrates the presence of strong pH buffering in the cytoplasm and also strong proton pumping that expels excess protons in a short period of time and maintains homeostatic pH while the external pH is several units higher or lower. In contrast to the effect of the strong acid, the addition of sorbic acid caused a prolonged intracellular acidification of hyphae, which did not recover during the 20 min following treatment. Sorbic acid is a weak acid that is membrane permeant in its undissociated (hydrophobic) form. Once in the cytosol, the weak acid will dissociate due to the higher pH in the cytoplasm compared to that of the external medium, thus trapping the membrane-impermeant charged acid anion. A proton also will be released into the cytoplasm during this process, resulting in cytoplasmic acidification. Cell-permeant weak acids have been used previously to clamp the intracellular pH of fungal and plant cells in pH measurement studies (1, 34).

Proton pumps are important for intracellular pH homeostasis. A BLAST analysis of the *A. niger* genome (35) has revealed that it contains seven predicted H^+-ATPases, of which five are P-ATPases, one a V-ATPase complex, and one an F-ATPase complex (5). All of these H^+ pumps could contribute to intracellular pH homeostasis by removing excess H^+ from the cytoplasm.

To investigate the role of ATPases in intracellular pH regulation, we used a range of ATPase inhibitors. We found that NEM, DCCD, and sodium azide caused the cytoplasmic pH to decrease by <0.1 pH unit. The ATPase inhibitor vanadate did not have much of an inhibitory effect, as was also shown by Sanders and Slayman (42), but this may be explained by the failure of vanadate to enter the cell (42, 45). However, one needs to be very cautious about overinterpreting the results obtained with ATPase inhibitors, because their specificity is questionable in fungi (e.g., Sussman and Slayman [44] showed that DCCD, which is often described as a V-ATPase inhibitor, also inhibited P-ATPases in *N. crassa*). Furthermore, it also is important to emphasize that the strongly active ATPase inhibitors will cause a large drop in cellular ATP levels, which will have numerous cellular side effects.

The protonophores CCCP and FCCP, also known as uncouplers of oxidative phosphorylation, (14), triggered irreversible intracellular acidification in *A. niger*. Our results are an improvement over those reported by Hesse et al. (20), who used NMR to measure intracellular pH. They reported a less-pronounced pH decrease following CCCP treatment, but with the protonophore at a concentration of 10 μM (as used in our study) they could no longer discriminate between the vacuolar and the cytoplasmic pH signal.

Pronounced, tip-focused cytoplasmic gradients are absent from growing hyphae. Using confocal ratio imaging, we were unable to demonstrate the presence of either pronounced tip-focused, longitudinal cytoplasmic pH gradient or cytoplasmic pH gradient across the apical 20-μm region of actively growing hyphae. Furthermore, gradients of this type were not observed in any hyphae growing in media ranging from pH 2.5 to 9.5. These results are consistent with those obtained from tip-growing hyphae of *N. crassa* and pollen tubes of *Lilium longiflorum* (13, 34). Al-Balwadi and Abercrombie (1) showed from estimates that the rate of proton diffusion, the buffer capacity of the cytoplasm, and rates of proton flux across membranes would tend to favor a pronounced change in pH (>0.1 pH unit) across distances of >25 μm. Previous reports of pronounced cytoplasmic pH gradients measured with fluorescent dyes in hyphae (25, 40, 41) were probably due to inferior imaging techniques and sequestration into acidic organelles (13, 34). Our results support the notion that cytoplasmic pH gradients are not a general feature of tip-growing cells and

argue against a central regulatory role of cytoplasmic pH gradients in tip growth.

Vacuolar pH can be imaged and measured with RaVC. RaVC was sequestered within tubular and spherical organelles, which were probably vacuoles, in older hyphae from 32-h-old cultures. Ratiometric measurements of RaVC within these putative vacuoles indicated that their pH values were 6.2 to 6.5, which are the same as previously reported for vacuoles of *A. niger* from NMR measurements (20). Measurements of vacuolar pH in budding yeast have been reported to be 5.6 to 6.1 (28) and 6.2 (37). To our knowledge, RaVC is the first probe that can be used as a recombinant vacuolar pH reporter in fungi.

ACKNOWLEDGMENTS

We thank A. Miyawaki, O. Griesbeck, and G. Miesenbock for the gifts of genes encoding Venus, Citrine, and pHluorin, respectively. We thank the computer engineer B. Knavs for helping develop software for the ratio image calculations.

This work was supported by the Slovenian Research Agency.

REFERENCES

1. **al-Baldawi, N. F., and R. F. Abercrombie.** 1992. Cytoplasmic hydrogen ion diffusion coefficient. Biophys. J. **61:**1470–1479.
2. **Alcántara-Sánchez, F., C. G. Reynaga-Pena, R. Salcedo-Hernández, and J. Ruiz-Herrera.** 2004. Possible role of ionic gradients in the apical growth of *Neurospora crassa*. Antonie van Leeuwenhoek **86:**301–311.
3. **Anand, S., and R. Prasad.** 1989. Rise in Intracellular pH is concurrent with "start" progression of *Saccharomyces cerevisiae*. J. Gen. Microbiol. **135:**2173–2179.
4. **Bachewich, C. L., and I. B. Heath.** 1997. The cytoplasmic pH influences hyphal tip growth and cytoskeleton-related organization. Fungal Genet. Biol. **21:**76–91.
5. **Bencina, M., T. Bagar, L. Lah, and N. Kraševec.** 2008. A comparative genomic analysis of calcium and proton signaling/homeostasis in *Aspergillus* species. Fungal Genet. Biol. doi:10.1016/j.fgb. 2008.07.019.
6. **Cano Abad, M. F., G. Di Benedetto, P. J. Magalhaes, L. Filippin, and T. Pozzan.** 2004. Mitochondrial pH monitored by a new engineered green fluorescent protein mutant. J. Biol. Chem. **297:**11521–11529.
7. **Cobbold, P. H., and T. J. Rink.** 1987. Fluorescence and bioluminescence measurement of cytoplasmic free calcium. Biochem. J. **248:**313–328.
8. **Elsliger, M. A., R. M. Wachter, G. T. Hanson, K. Kallio, and S. J. Remington.** 1999. Structural and spectral response of green fluorescent protein variants to changes in pH. Biochemistry **38:**5296–5301.
9. **Feige, J. N., D. Sage, W. Wahli, B. Desvergne, and L. Gelman.** 2005. PixFRET, an ImageJ plug-in for FRET calculation that can accommodate variations in spectral bleed-throughs. Microsc. Res. Tech. **68:**51–88.
10. **Felle, H. H.** 1996. Control of cytoplasmic pH under anoxic conditions and its implication for plasma membrane proton transport in *Medicago sativa* root hairs. J. Exp. Bot. **47:**967–973.
11. **Fernández-Abalos, J. M., H. Fox, C. Pitt, B. Wells, and J. H. Doonan.** 1998. Plant-adapted green fluorescent protein is a versatile vital reporter for gene expression, protein localization and mitosis in the filamentous fungus, *Aspergillus nidulans*. Mol. Microbiol. **27:**121–130.
12. **Fricker, M. D., A. Parsons, M. Tlalka, E. Blancaflor, S. Gilroy, A. Meyer, and C. Plieth.** 1999. Fluorescent probes for living plant cells, p. 35–84. *In* C. Hawes and B. Satiai-Jeunemaitre (ed.), Plant cell biology: a practical approach, 2nd ed. University Press Oxford, Oxford, United Kingdom.
13. **Fricker, M. D., N. S. White, and G. Obermeyer.** 1997. pH gradients are not associated with tip growth in pollen tubes of *Lilium longiflorum*. J. Cell Sci. **110:**1729–1740.
14. **Galkina, S. I., G. F. Sud'ina, and T. Klein.** 2006. Metabolic regulation of neutrophil spreading, membrane tubulovesicular extensions (cytonemes) formation and intracellular pH upon adhesion to fibronectin. Exp. Cell Res. **312:**2568–2579.
15. **Griesbeck, O., G. S. Baird, R. E. Campbell, D. A. Zacharias, and R. Y. Tsien.** 2001. Reducing the environmental sensitivity of yellow fluorescent protein. Mechanism and applications. J. Biol. Chem. **276:**29188–29194.
16. **Grynkiewicz, G., M. Poenie, and R. Y. Tsien.** 1985. A new generation of Ca^{2+} indicators with greatly improved fluorescence properties. J. Biol. Chem. **260:**3440–3450.
17. **Hanson, G. T., T. B. McAnaney, E. S. Park, M. E. Rendell, D. K. Yarbrough, S. Chu, L. Xi, S. G. Boxer, M. H. Montrose, and S. J. Remington.** 2002. Green fluorescent protein variants as ratiometric dual emission pH sensors. 1. Structural characterization and preliminary application. Biochemistry **41:**15477–15488.
18. **Haq, I. U., S. Ali, and M. A. Qadeer.** 2005. Influence of dissolved oxygen concentration on intracellular pH for regulation of *Aspergillus niger* growth rate during citric acid fermentation in a stirred tank bioreactor. Int. J. Biol. Sci. **1:**34–41.
19. **Hesse, S. J. A., G. J. G. Ruijter, C. Dijkema, and J. Visser.** 2000. Measurement of intracellular (compartmental) pH by ^{31}P NMR in *Aspergillus niger*. J. Biotechnol. **77:**5–15.
20. **Hesse, S. J. A., G. J. G. Ruijter, C. Dijkema, and J. Visser.** 2002. Intracellular pH homeostasis in the filamentous fungus *Aspergillus niger*. Eur. J. Biochem. **269:**3485–3494.
21. **Hickey, P. C., S. R. Swift, M. G. Roca, and N. D. Read.** 2005. Live-cell imaging of filamentous fungi using vital fluorescent dyes and confocal microscopy, p. 63–87. *In* T. Savidge and C. Pothoulakis (ed.), Methods in microbiology. Elsevier, London, United Kingdom.
22. **Hickey, P. C., and N. D. Read.** 2009. Imaging living cells of *Aspergillus* in vitro. Med. Mycol. **2:**1–10.
23. **Jankowski, A., J. H. Kim, R. F. Collins, R. Daneman, P. Walton, and S. Grinstein.** 2001. In situ measurements of the pH of mammalian peroxisomes using the fluorescent protein pHluorin. J. Biol. Chem. **276:**48748–48753.
24. **Jernejc, K., and M. Legisa.** 2004. A drop of intracellular pH stimulates citric acid accumulation by some strains of *Aspergillus niger*. J. Biotechnol. **112:**289–297.
25. **Jolicoeur, M., S. Germette, M. Gaudette, M. Perrier, and G. Becard.** 1998. Intracellular pH in arbuscular mycorrhizal fungi. A symbiotic physiological marker. Plant Physiol. **116:**1279–1288.
26. **Karagiannis, J., and P. G. Young.** 2001. Intracellular pH homeostasis during cell-cycle progression and growth state transition in *Schizosaccharomyces pombe*. J. Cell Sci. **114:**2929–2941.
27. **Legiša, M., and M. Mattey.** 2007. Changes in primary metabolism leading to citric acid overflow in *Aspergillus niger*. Biotechnol. Lett. **29:**181–190.
28. **Martínez-Muñoz, G. A., and P. Kane.** 2008. Vacuolar and plasma membrane proton pumps collaborate to achieve cytosolic pH homeostasis in yeast. J. Biol. Chem. **283:**20309–20319.
29. **Miesenböck, G., D. A. DeAngelis, and J. E. Rothman.** 1998. Visualizing secretion and synaptic transmission with pH sensitive green fluorescent proteins. Nature **394:**192–195.
30. **Millington, M., G. J. Grindlay, K. Altenbach, R. K. Neely, W. Kolch, M. Bencina, N. D. Read, A. C. Jones, D. T. Dryden, and S. W. Magennis.** 2007. High-precision FLIM-FRET in fixed and living cells reveals heterogeneity in a simple CFP-YFP fusion protein. Biophys. Chem. **127:**155–164.
31. **Nakamura, Y., T. Gojobori, and T. Ikemura.** 2000. Codon usage tabulated from the international DNA sequence databases: status for the year. Nucleic Acids Res. **28:**292.
32. **Nelson, N., N. Perzov, A. Cohen, K. Hagai, V. Padler, and H. Nelson.** 2000. The cellular biology of proton-motive force generation by V-ATPases. J. Exp. Biol. **203:**89–95.
33. **Parton, R. M., and N. D. Read.** 1999. Calcium and pH imaging in living cells, p. 211–264. *In* A. J. Lacey (ed.), Light microscopy in biology, 2nd ed. Oxford University Press, Oxford, United Kingdom.
34. **Parton, R. M., S. Fischer, R. Malhó, O. Papasouliotis, T. C. Jelitto, T. Leonard, and N. D. Read.** 1997. Pronounced cytoplasmic pH gradients are not required for tip growth in plant and fungal cells. J. Cell Sci. **110:**1187–1198.
35. **Pel, H. J., J. H. de Winde, D. B. Archer, P. S. Dyer, G. Hofmann, P. J. Schaap, G. Turner, R. P. de Vries, R. Albang, K. Albermann, M. R. Andersen, J. D. Bendtsen, J. A. Benen, M. van den Berg, S. Breestraat, M. X. Caddick, R. Contreras, M. Cornell, P. M. Coutinho, E. G. Danchin, A. J. Debets, P. Dekker, P. W. van Dijck, A. van Dijk, L. Dijkhuizen, A. J. Driessen, C. d'Enfert, S. Geysens, C. Goosen, G. S. Groot, P. W. de Groot, T. Guillemette, B. Henrissat, M. Herweijer, J. P. van den Hombergh, C. A. van den Hondel, R. T. van der Heijden, R. M. van der Kaaij, F. M. Klis, H. J. Kools, C. P. Kubicek, P. A. van Kuyk, J. Lauber, X. Lu, M. J. van der Maarel, R. Meulenberg, H. Menke, M. A. Mortimer, J. Nielsen, S. G. Oliver, M. Olsthoorn, K. Pal, N. N. van Peij, A. F. Ram, U. Rinas, J. A. Roubos, C. M. Sagt, M. Schmoll, J. Sun, D. Ussery, J. Varga, W. Vervecken, P. J. van de Vondervoort, H. Wedler, H. A. Wösten, A. P. Zeng, A. J. van Ooyen, J. Visser, and H. Stam.** 2007. Genome sequencing and analysis of the versatile cell factory *Aspergillus niger* CBS 513.88. Nat. Biotechnol. **25:**221–231.
36. **Plumridge, A., S. J. Hesse, A. J. Watson, K. C. Lowe, M. Stratford, and D. B. Archer.** 2004. The weak acid preservative sorbic acid inhibits conidial germination and mycelial growth of *Aspergillus niger* through intracellular acidification. Appl. Environ. Microbiol. **70:**3506–3511.
37. **Preston, R. A., R. F. Murphy, and E. W. Jones.** 1989. Assay of vacuolar pH in yeast and identification of acidification-defective mutant. Proc. Natl. Acad. Sci. USA **86:**7027–7031.
38. **Putnam, R.** 1998. Intracellular pH regulation, p. 293–305. *In* N. Sperelakis (ed.), Cell physiology source book. Academic Press, San Diego, CA.
39. **Rekas, A., J. R. Alattia, T. Nagai, A. Miyawaki, and M. Ikura.** 2002. Crystal structure of Venus, a yellow fluorescent protein with improved maturation and reduced environmental sensitivity. J. Biol. Chem. **277:**50573–50578.

40. **Robson, G. D., E. Prebble, A. Rickers, S. Hosking, D. W. Denning, A. P. J. Trinci, and W. Robertson.** 1996. Polarized growth of fungal hyphae is defined by an alkaline pH gradient. Fungal Genet. Biol. **20:**289–298.
41. **Roncal, T., U. O. Ugalde, and A. Irastorza.** 1993. Calcium-induced conidiation in *Penicillium cyclopium*: calcium triggers cytosolic alkalinization at the hyphal tip. J. Bacteriol. **175:**879–886.
42. **Sanders, D., and C. L. Slayman.** 1982. Control of intracellular pH: predominant role of oxidative metabolism, not proton transport in the eukaryotic microorganism *Neurospora*. J. Gen. Physiol. **80:**377–402.
43. **Schulte, A., I. Lorenzen, M. Bottcher, and C. Plieth.** 2006. A novel fluorescent pH probe for expression in plants. Plant Methods **2:**7–20.
44. **Sussman, M. R., and C. W. Slayman.** 1983. Modification of the *Neurospora crassa* plasma membrane [H+]-ATPase with N,N′-dicyclohexylcarbodiimide. J. Biol. Chem. **258:**1839–1843.
45. **van Der Heyden, N., G. Benaim, and R. Docampo.** 1996. The role of a H^+-ATPase in the regulation of cytoplasmic pH in Trypanosoma cruzi epimastigotes. Biochem. J. **318:**103–109.
46. **Zaccolo, M., and T. Pozzan.** 2000. Imaging signal transduction in living cells with GFP-based probes. IUBMB Life **49:**375–379.
47. **Zacharias, D. A., J. D. Violin, A. C. Newton, and R. Y. Tsien.** 2002. Partitioning of lipid-modified monomeric GFPs into membrane microdomains of live cells. Science **296:**913–916.